

COLOR-OCTET SCALARS OF $N = 2$ SUPERSYMMETRY AT THE LHCS. Y. Choi¹, M. Drees², J. Kalinowski³, J. M. Kim², E. Popenoda⁴ and P. M. Zerwas^{4,5}¹ Department of Physics and RIPC, Chonbuk National University, Jeonju 561-756, Korea² Physikalisches Inst. der Univ. Bonn, D-53115 Bonn, Germany and
Bethe Center for Theoretical Physics, Univ. Bonn, D-53115 Bonn, Germany³ Physics Department, University of Warsaw, 00681 Warsaw, Poland and
Theory Division, CERN, CH-1211 Geneva 23, Switzerland⁴ Inst. Theor. Physik E, RWTH Aachen U., D-52074 Aachen, Germany⁵ Deutsches Elektronen-Synchrotron DESY, D-22603 Hamburg, Germany and
Laboratoire de Physique Théorique, U. Paris-Sud, F-91405 Orsay, France

(Dated: August 11, 2024)

The color gauge hypermultiplet in $N = 2$ supersymmetry consists of the usual $N = 1$ gauge vector/gaugino supermultiplet, joined with a novel gaugino/scalar supermultiplet. Large cross sections are predicted for the production of pairs of the color-octet scalars [sgluons] at the LHC: $gg \rightarrow q\bar{q}$. Single production is possible at one-loop level, but the $gg \rightarrow$ amplitude vanishes in the limit of degenerate L and R squarks. When kinematically allowed, decays predominantly into two gluinos, whose cascade decays give rise to a burst of eight or more jets together with four LSP's as signature for pair events at the LHC. can also decay into a squark-antisquark pair at tree level. At one-loop level decays into gluons or a $t\bar{t}$ pair are predicted, generating exciting resonance signatures in the final states. The corresponding partial widths are very roughly comparable to that for three body final states mediated by one virtual squark at tree level.

1. INTRODUCTION

The pairwise production of supersymmetric squarks and gluinos at the LHC leads to final states that contain two to four hard jets [plus somewhat softer jets from QCD radiation and/or decays of heavier neutralinos and charginos] and missing transverse momentum generated by two LSP's. These signatures are typical for $N = 1$ supersymmetry [1, 2, 3] as specified in the Minimal Supersymmetric Standard Model [MSSM]. However, in alternative realizations of supersymmetry the final-state topology could be rather different. In order to exemplify this point, we have adopted an $N = 1/N = 2$ hybrid model, cf. Ref. [4, 5, 6], in which supersymmetry characteristics are quite different from the MSSM. Assuming the $N = 2$ mirror (s)fermions to be very heavy in order to avoid chirality problems, the hybrid model expands to $N = 2$ only in the gaugino sector. The QCD sector is built up by the usual $N = 1$ gluon/gluino supermultiplet, joined with an additional gluino/scalar supermultiplet. [Similarly, the electroweak sector is supplemented by additional $SU(2)_L$ and $U(1)_Y$ supermultiplets; this sector will not be discussed here.] For the sake of simplicity we will disregard in the analysis mass splittings of the scalar fields and we assume equal masses for the usual and the novel gluinos which, as a result, can be combined to a common Dirac field, see Refs. [5, 6, 7]. Since the experimental consequences of variations involving a larger set of parameters are rather obvious, they will not be discussed in this letter.

The novel scalar color-octet fields [which may be called scalar gluons¹, or contracted to sgluons [8]] can be produced in pairs:

$$gg; qq \rightarrow \text{sgluons} \quad (1.1)$$

The color-octet sgluons are R-parity even, and thus can also be produced singly in gluon-gluon or quark-antiquark collisions, albeit through loop processes only:

$$gg; qq \rightarrow \text{sgluons} \quad (1.2)$$

However, as we will show, the corresponding matrix elements vanish in the limit of degenerate L and R squarks. Moreover, single sgluon production in quark-antiquark collisions proceeds through a chirality-flip process that is suppressed, strongly in practice, by the quark mass.

At tree level, sgluons can decay either into (real or virtual) gluino or squark pairs,

$$\begin{aligned} \text{sgluons} &\rightarrow gg; \text{sgluons} \rightarrow qq + \tilde{\chi}^0; \\ \text{sgluons} &\rightarrow qq; \text{sgluons} \rightarrow qq + \tilde{\chi}^{\pm}; \end{aligned} \quad (1.3)$$

where $\tilde{\chi}$ denotes electroweak neutralinos or charginos. At one-loop level, sgluons can also decay into top-quark or gluon pairs:

$$\begin{aligned} \text{sgluons} &\rightarrow tt; \text{sgluons} \rightarrow bb + W^{\pm}; \\ \text{sgluons} &\rightarrow gg; \end{aligned} \quad (1.4)$$

Apart from the last mode, these lead to spectacular signatures for sgluons pair production at the LHC, e.g.

$$\begin{aligned} pp &\rightarrow 8 \text{ jets} + 4 \text{ LSP}^0\text{s}; \\ pp &\rightarrow tttt; \end{aligned} \quad (1.5)$$

In the first case a burst of eight almost isotropically distributed hard jets is generated in sgluons -pair production, even not counting QCD stray jets nor possible $\tilde{\chi}$ decay products, and a large amount of missing energy. Alternatively, four top (anti)quarks are predicted by the second mechanism. These signatures are very different from the usual MSSM topologies and raise exciting new experimental questions. Likewise, single sgluons production followed by gluon-pair decays generates novel resonance signatures foreign to $N=1$ supersymmetry.

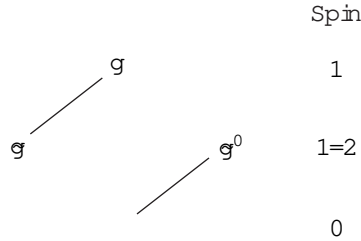
Apart from Ref. [8], the possibility that there might exist $SU(3)_C$ octet scalars within reach of the LHC has recently been discussed in different context in Refs. [9]. While the tree-level cross sections for the pair production of these scalars at the LHC are the same in all these scenarios [up to trivial multiplicity factors], the possibilities of single production, as well as the decay modes and experimental signatures of the scalars in both channels, are quite different in our case and Ref. [8] from those discussed earlier.

This note is divided into two parts. In the next section the theoretical basis of the $N=1/N=2$ hybrid model will be recapitulated briefly, and the loop-induced gg and qq couplings will be discussed. The third section is devoted to the phenomenology of sgluons -pair production and cascade decays, followed by a short analysis of single sgluons production in gluon fusion.

¹ Not to be confused with the scalar gluons that were discussed as carriers of the strong force in alternatives to QCD constructed in the 1970's.

2. THEORETICAL BASIS: GAUGE HYPER-MULTIPLETS AND SCALARS

As noted earlier, the $N=2$ QCD hyper-multiplet can be decomposed into the usual $N=1$ octet gluon/gluino multiplet $\hat{\mathcal{G}} = \{g, \tilde{g}\}$ plus an $N=1$ octet multiplet $\hat{\mathcal{G}}^0 = \{g^0, \tilde{g}^0\}$ of extra gluinos and scalar fields. Schematically, the QCD hyper-multiplet is described by a diamond plot,



where the first, second and third row corresponds to spin 1, 1/2 and 0 states. The $N=1$ super fields are represented by the two pairs connected by the thin lines. The \tilde{g}^0 field carries positive R-parity.

The only gauge invariant term in the $N=1$ superpotential containing the new gluino/sgluon super field $\hat{\mathcal{G}}^0$ is a mass term,

$$W_{\mathcal{G}^0} = \frac{1}{2} M_3^0 \hat{\mathcal{G}}^{0a} \hat{\mathcal{G}}^{0a}; \tag{2.1}$$

where we have adopted the notation of Ref. [5]. The only supersymmetric interactions involving $\hat{\mathcal{G}}^0$ are thus QCD gauge interactions plus gauge strength \tilde{g}^0 Yukawa-type interactions [5]. In a full $N=2$ theory, there would also be couplings between $\hat{\mathcal{G}}^0$ and the $N=2$ partners of the usual matter super fields; however, in our hybrid construction we assume the latter to be decoupled from TeV scale physics.

The masses of the new scalars are determined by the superpotential (2.1) plus soft breaking terms [10]

$$\mathcal{L}_{\text{soft}} = -m^2 \sum_i \tilde{Q}_i \tilde{Q}_i - m^2 \sum_j \tilde{U}_j \tilde{U}_j + h.c. - g_s M_3^D \sum_a \frac{1}{2} \tilde{g}^0_a \sum_q (\tilde{Q}_{L_i} \tilde{Q}_{L_j} - \tilde{Q}_{R_i} \tilde{Q}_{R_j}) + h.c.; \tag{2.2}$$

where g_s is the strong coupling constant and T^a are the Gell-Mann $SU(3)_C$ matrices. The parameter M_3^D is the Dirac gluino mass connecting \tilde{g}^0 with the usual gluino \tilde{g} [5]. If the supersymmetry breaking is spontaneous, the Dirac gluino mass also gives rise to a supersymmetry breaking trilinear scalar interaction between \tilde{g}^0 and the MSSM squarks, as shown in Eq. (2.2); note that L and R squarks contribute with opposite signs as demanded by the general form of the super-QCD D-terms [differing from the first version of Ref. [8] with far reaching phenomenological consequences].² As noted above, we will set $m^2 = 0$ in this discussion, so that the physical mass of the complex scalar octet is

$$M = \sqrt{M_3^D{}^2 + m^2}; \tag{2.3}$$

For given mean mass, a nonzero m^2 generating a mass splitting of the scalar fields would increase the total cross section for the production of the new scalars.

In the simplest realization the two gluinos, \tilde{g} and \tilde{g}^0 , are not endowed with individual masses [i.e. $M_3^0 = 0$] but they are coupled by the mass parameter M_3^D in a purely off-diagonal mass matrix.³ In this configuration the two

² If one allows oneself the freedom to break supersymmetry explicitly, but softly, the coefficients of the $\tilde{g}\tilde{g}$ interactions would be arbitrary, and could even be set to zero; this would, however, not be stable against radiative corrections.
³ Note that this Dirac mass term must be nonzero, since otherwise the lightest member of the super field $\hat{\mathcal{G}}$ would be stable. In contrast, scenarios where the diagonal Majorana entries of the gluino mass matrix vanish are perfectly acceptable.

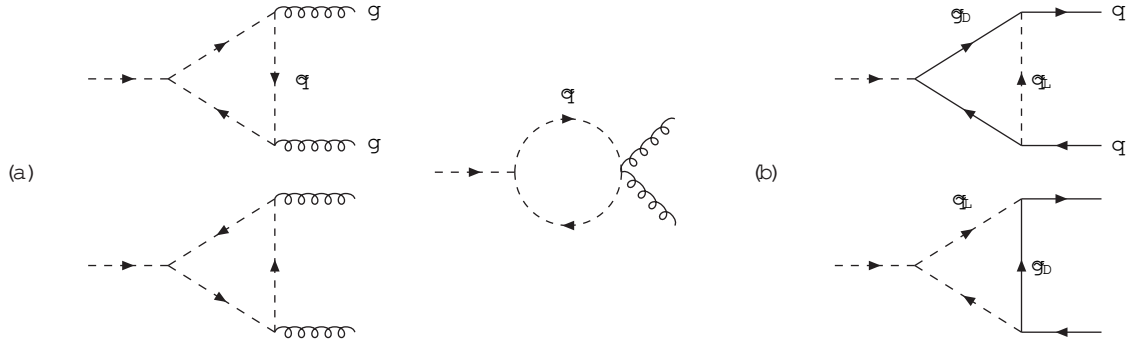


Figure 1: Diagrams for (a) the effective gg vertex built up by squark loops; (b) the effective qq vertex with L squarks and gluinos (the coupling to R squarks being mediated by the charge-conjugate Dirac gluinos).

Majana gluinos can be combined to a 4-component Dirac gluino field \mathfrak{G}_D as

$$\mathfrak{G}_D = \mathfrak{G}_R + \mathfrak{G}_L^0; \quad (2.4)$$

with the mass eigenvalue given by $M_{\frac{D}{3}}$ cf. Ref. [5]. The couplings of this Dirac field \mathfrak{G}_D to the $-$ field and to the squark and quark fields are summarized in the interaction Lagrangians

$$L_{\mathfrak{G}_D \mathfrak{G}_B} = \frac{P}{2} i g_s f^{abc} \overline{\mathfrak{G}_D^a} \mathfrak{G}_D^b \mathfrak{G}_B^c + \text{h.c.}; \quad (2.5)$$

$$L_{\mathfrak{G}_D q\bar{q}} = \frac{P}{2} g_s \left[\frac{a}{Q_L} \mathfrak{G}_D^a \mathfrak{G}_L + \frac{a^T}{Q_R} \mathfrak{G}_D^a \mathfrak{G}_R \right] + \text{h.c.}; \quad (2.6)$$

where $\mathfrak{G}_D^c = (\mathfrak{G}_R + \mathfrak{G}_L)$ is the charge-conjugate 4-component Dirac gluino [5], f^{abc} are the $SU(3)_C$ structure constants and a^a are the Gell-Mann matrices. In addition, the sgluon fields couple to gluons in tri- and quattro-linear vertices as prescribed by gauge theories for scalar octet fields, i.e. proportional to the octet self-adjoint $SU(3)_C$ representation F . As a result, at tree level pairs can be produced in gluon collisions as well as in $q\bar{q}$ annihilation, but single production of \mathfrak{G} 's is not possible.

Even at the one-loop level, gluino loops do not contribute to the gg coupling, due to the Bose symmetry of the gluons. The coupling is even in the 4-momenta under gluon exchange but it is odd, on the other hand, due to the antisymmetric octet matrix elements f^{abc} in color space. [Note that $SU(3)_C$ singlet particles, like Higgs bosons, couple symmetrically to gluons, by contrast.] Actually, the coupling of the octet sgluon to any number of gluons is forbidden in the general softly broken $N=2$ pure gauge theory with two Majana gluinos [which may or may not be combined to a single Dirac gluino] because the totally antisymmetric factor f^{abc} forces the sgluon to couple only to two different Majana gluinos, while gluons always couple to diagonal Majana gluino pairs.

However, \mathfrak{G} can couple non-trivially to gluon pairs and quark-antiquark pairs through triangle diagrams involving squark lines. Characteristic examples are depicted in Fig.1. In parallel to the interaction Lagrangian it turns out that all L- and R-squark contributions to the couplings come with opposite signs so that they cancel each other for mass degenerate squarks. In addition, the quark-antiquark coupling is suppressed by the quark mass as evident from general chirality rules.

Comment. Before discussing the phenomenological implications, let us note that the presence of new fields in the $N=1/N=2$ hybrid model affects the renormalization group (RG) running of gauge couplings above the weak scale; to one-loop order,

$$\frac{d}{d \log(Q^2)} \frac{1}{g_i^2(Q^2)} = \frac{b_i}{2}; \quad (2.7)$$

The coefficients b_i for the non-Abelian group factors $SU(N_i)$ receive in the hybrid model contributions in addition to MSSM,

$$b_i = b_i^{\text{MSSM}} + \frac{2}{3}N_i + \frac{1}{3}N_i; \quad (2.8)$$

where the second term comes from the new M adjoint fermions ψ^0 and the third from the complex scalars; the running of the $U(1)_Y$ coupling remains unaffected at one-loop order. As a result, gauge coupling unification and the prediction of the weak mixing angle are lost; instead, the couplings g_i and g_j meet at different points $M_{X,ij}$, all of which lie above the Planck scale. Possible solutions to this problem would be to add fields to the theory so that the new fields fall in complete GUT multiplets [11], or to allow a different normalization for $U(1)_Y$ [12], or to contemplate different unification patterns [10], etc. Since in this letter we are interested in the low-energy phenomenology of the color-octet scalars, we will not delve into this subject any further.

3. PHENOMENOLOGY OF COLOR-OCTET SCALARS AT THE LHC

3.1. Decays

At tree level the ψ particles can decay to a pair of Dirac gluinos \tilde{g} or into a pair of squarks, with one or both of these particles being potentially virtual when $M < 2m_{\tilde{g}}$; $2m_{\tilde{q}}$. For on-shell decays and assuming pure Dirac gluinos the partial widths are

$$\begin{aligned} \Gamma(\psi \rightarrow \tilde{g}\tilde{g}) &= \frac{3}{4} \frac{sM}{M} g^2 (1 + \frac{2}{g}); \\ \Gamma(\psi \rightarrow \tilde{q}_a\tilde{q}_a) &= \frac{s}{4} \frac{M^D}{M} \frac{f^2}{M} g_a^2; \end{aligned} \quad (3.1)$$

where g, g_a are the velocities of \tilde{g}, \tilde{q}_a ($a = L; R$). In the presence of non-trivial $\tilde{q}_L - \tilde{q}_R$ mixing the subscripts $L; R$ in the second Eq.(3.1) have to be replaced by 1;2 labeling the mass eigenstates, and the contribution from this flavor is suppressed by a factor $\cos^2(2\theta_q)$; the mixing angle is defined via the decomposition of the lighter mass eigenstate $\tilde{q}_1 = \cos\theta_q \tilde{q}_L + \sin\theta_q \tilde{q}_R$. In addition, decays into $\tilde{q}_1\tilde{q}_2$ and $\tilde{q}_1\tilde{q}_2$ are possible, with the coefficient $\sin^2(2\theta_q)$ and with the velocity g_a replaced by the phase-space function $\sqrt{1 - 2(m_{\tilde{q}_1}^2 + m_{\tilde{q}_2}^2)/M^2}$. The gluinos subsequently decay to quarks and squarks, again either real or virtual, and the squarks to quarks and charginos/neutralinos tumbling eventually down to the LSP.

On the other hand, the trilinear interaction in Eq.(2.2) gives rise to an effective gg coupling via squark loops, Fig. 1 (a), leading to the partial decay width

$$\Gamma(\psi \rightarrow gg) = \frac{5}{384} \frac{s^3}{M^2} \frac{M^D}{M} \frac{f^2}{M} X_q^2 [\tilde{q}_L f(\tilde{q}_L) + \tilde{q}_R f(\tilde{q}_R)]; \quad (3.2)$$

with $X_{L;R} = 4m_{\tilde{q}_{L;R}}^2/M^2$ and [13]

$$f(x) = \begin{cases} \frac{8}{3} \ln \frac{1+x}{1-x} - \frac{1}{x} & \text{for } x > 1; \\ \frac{1}{4} \ln \frac{1+x}{1-x} - \frac{1}{x} & \text{for } x < 1; \end{cases} \quad (3.3)$$

In the presence of nontrivial $\tilde{q}_L - \tilde{q}_R$ mixing, the subscripts $L; R$ in Eq.(3.2) again have to be replaced by 1;2 labeling the mass eigenstates, and the contribution from this flavor is suppressed by a factor $\cos(2\theta_q)$ multiplying the term in square parentheses. Note that the gg coupling vanishes in the limit of degenerate L and R squarks.

Furthermore, the field couples to quark-antiquark pairs (in principle). By standard helicity arguments, this chirality- γ_5 coupling is suppressed however by the quark mass. For pure Dirac gluinos, the triangle diagrams, Fig. 1 (b), either with two internal gluino lines and one squark line or with two internal squark lines and one gluino line again vanish for degenerate L and R squarks. The resulting partial width can be written as

$$\Gamma(\tilde{g} \rightarrow q\bar{q}) = \frac{9}{128} \frac{g_s^3}{M} \frac{M_3^D}{M} \frac{f m_q^2}{M} \left[C_L^2 + 4m_q^2 \mathcal{I}_S + M^2 \mathcal{I}_P \right] ; \quad (3.4)$$

The loop integrals for the effective scalar (S) and pseudoscalar (P) couplings are given by

$$\begin{aligned} \mathcal{I}_S &= \int_0^1 dx \int_0^{1-x} dy (1-x-y) \frac{1}{C_L} \frac{1}{C_R} + \frac{1}{9} (x+y) \frac{1}{D_L} \frac{1}{D_R} ; \\ \mathcal{I}_P &= \int_0^1 dx \int_0^{1-x} dy \frac{1}{C_L} \frac{1}{C_R} ; \end{aligned} \quad (3.5)$$

where we have defined ($a = L; R$)

$$\begin{aligned} C_a &= (x+y) M_3^D \frac{f}{M} + (1-x-y) m_{\tilde{q}_a}^2 - xy M^2 - (x+y)(1-x-y) m_{\tilde{g}}^2 ; \\ D_a &= (1-x-y) M_3^D \frac{f}{M} + (x+y) m_{\tilde{q}_a}^2 - xy M^2 - (x+y)(1-x-y) m_{\tilde{g}}^2 ; \end{aligned} \quad (3.6)$$

$\mathcal{I}_{S,P}$ can also be expressed in terms of standard Passarino-Veltman functions [14], e.g. $\mathcal{I}_P = C_{0L} - C_{0R}$, with $C_{0L;R} = C_0(M_3^D \frac{f}{M}; m_{\tilde{q}_{L;R}}^2; M_3^D \frac{f}{M}; m_{\tilde{q}}^2; m_{\tilde{g}}^2; M^2)$. In the presence of nontrivial \tilde{q}_L - \tilde{q}_R mixing, the subscripts L;R in Eq.(3.5) have to be replaced by 1;2 labeling the squark mass eigenstates, and the contribution from this flavor to the double integrals is suppressed by a factor $\cos(2\varphi_q)$. Note that $\mathcal{I}_S = \mathcal{I}_P = 0$ if $m_{\tilde{q}_L} = m_{\tilde{q}_R}$. In the presence of \tilde{q}_L - \tilde{q}_R mixing this cancellation is no longer exact for two non-degenerate Majorana gluinos.

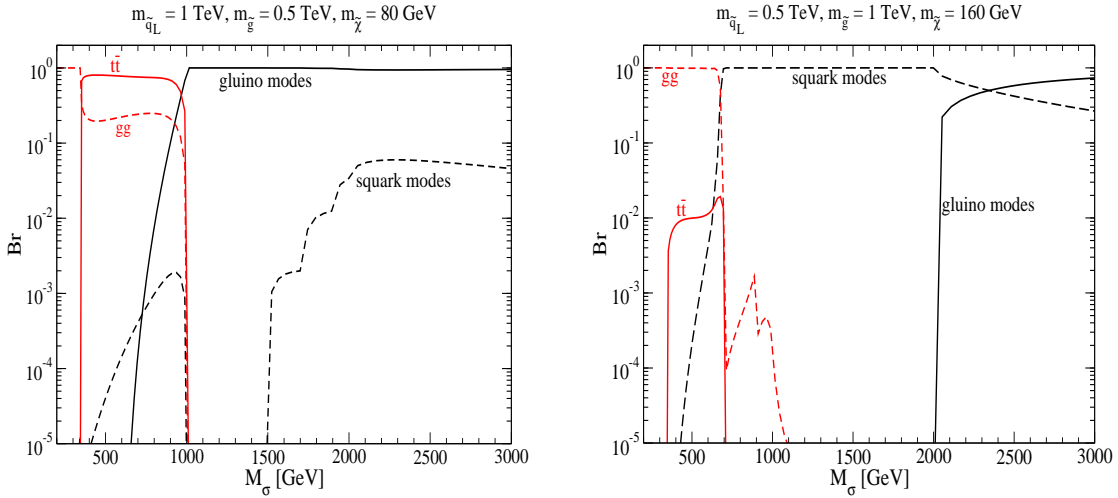


Figure 2: Branching ratios for $\tilde{g} \rightarrow q\bar{q}$ decays, for $m_{\tilde{q}_L} = 2m_{\tilde{g}} = 1$ TeV (Left) and $m_{\tilde{g}} = 2m_{\tilde{q}_L} = 1$ TeV (Right). In both cases we assumed a neutralino mass $m_{\tilde{\chi}} = 0.16m_{\tilde{g}}$, and moderate squark mass splitting: $m_{\tilde{q}_R} = 0.95m_{\tilde{q}_L}$; $m_{\tilde{t}_L} = 0.9m_{\tilde{q}_L}$; $m_{\tilde{t}_R} = 0.8m_{\tilde{q}_L}$, with \tilde{t}_L - \tilde{t}_R mixing determined by $X_t = m_{\tilde{q}_L}$.

The corresponding 2-body branching ratios are compared to those for tree-level decays in Fig.2. Here we assume moderate mass splitting between the L and R squarks of the ve light flavors, and somewhat greater for soft breaking \tilde{t} masses: $m_{\tilde{q}_R} = 0.95m_{\tilde{q}_L}$; $m_{\tilde{t}_L} = 0.9m_{\tilde{q}_L}$; $m_{\tilde{t}_R} = 0.8m_{\tilde{q}_L}$. We parameterize the off-diagonal element of the squared \tilde{t} mass matrix as $X_t m_{\tilde{t}}$, and take $X_t = m_{\tilde{q}_L}$. We again assume the gluino to be a pure Dirac state, i.e. $m_{\tilde{g}} = M_3^D \frac{f}{M}$.

Even for this small mass splitting, the loop decays into two gluons and, if kinematically allowed, a tt pair always dominate over tree-level four-body decays $\tilde{g} \rightarrow q\bar{q}q\bar{q}$ (which is part of the "gluino modes" in Fig.2) and $\tilde{g} \rightarrow q\bar{q}q\bar{q}$

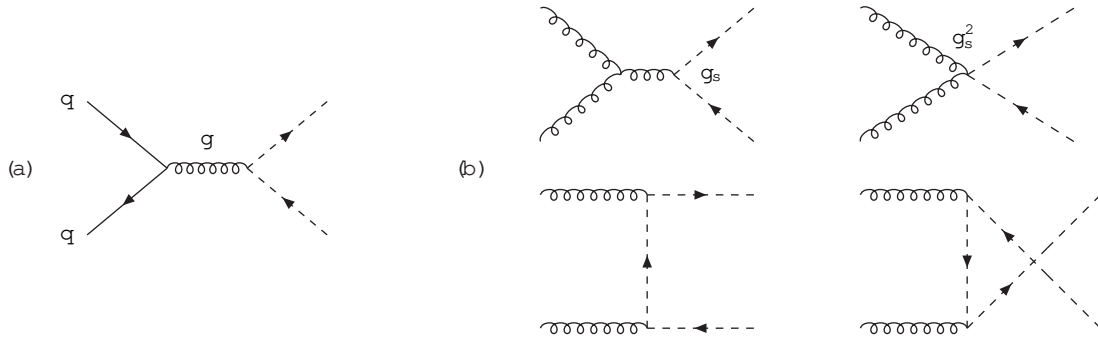


Figure 3: Feynman diagrams for signa-pair production in quark annihilation (a) and gluon fusion (b).

(which is part of the "squark modes"). For simplicity we evaluated these higher order tree-level decays for a photino LSP state, with mass $0.16m_g$. $SU(2)_L$ gauginos have larger couplings to doublet squarks, but are also expected to be heavier. Including them in the final state would at best increase the partial widths for four-body final states by a factor of a few, which would still leave them well below the widths for the loop induced decays. On the other hand, the partial width for the tree-level three-body decays $\tilde{q}q\tilde{q}$; $\tilde{q}q\tilde{q}$ can be comparable to that for the loop-induced decays if M is not too much smaller than $2m_q$.

Figure 2 also shows that the ordering between the two loop-induced decay modes for $M > 2m_t$ depends on the values of various soft breaking parameters. Increasing the gluino mass increases the $\tilde{q}q\tilde{q}$ coupling and hence the partial width into two gluons which is due to pure squark loops. On the other hand, the tt partial width, which is due to mixed squark-gluino loops, decreases rapidly with increasing gluino mass. The increase of the $\tilde{q}q\tilde{q}$ couplings is over-compensated by the gluino mass dependence of the propagators. For $M_{3/2}^D > m_q$ the loop functions $I_{S,P}$ are additionally suppressed since then $C_L \neq C_R$; $D_L \neq D_R$ up to corrections of $O(m_q^2/M_{3/2}^D)$. [A similar cancellation also occurs for $M^2 \sim m_q^2$, for both the gg and tt couplings.] In total, the tt final state will dominate for small gluino mass and the gg final state for large gluino mass. Moreover, as noted earlier, the partial width into both gluons and quarks vanishes for exact degeneracy between L and R squarks.

Not surprisingly, the two-body final states of Eq. (3.1) that are accessible at tree level will dominate if they are kinematically allowed. Note that well above all thresholds the partial width into gluinos always dominates, since it grows $\propto M$ while the partial width into squarks asymptotically scales like $1/M$. This is a result of the fact that the supersymmetry breaking $\tilde{q}q\tilde{q}$ coupling has mass dimension 1, while the supersymmetric $gg\tilde{q}$ coupling is dimensionless.

3.2. $\tilde{q}q$ -Pair Production at the LHC

As summarized in the preceding section, the phenomenological analysis will be carried out for a complex color-octet fields without mass splitting between the real and imaginary components. The Feynman diagrams for the two parton processes $gg \rightarrow \tilde{q}q$; $q\bar{q} \rightarrow \tilde{q}q$ are displayed in Fig. 3. They are identical (modulo color factors) to squark-pair production [15, 16] if initial and final-state flavors are different.

The total cross sections for the two parton processes are easy to calculate:

$$\sigma(q\bar{q} \rightarrow \tilde{q}q) = \frac{4}{9s} \frac{s^2}{s^3}; \quad (3.7)$$

$$\sigma(gg \rightarrow \tilde{q}q) = \frac{15}{8s} \frac{s^2}{s} \left[1 + \frac{34}{5} \frac{M^2}{s} - \frac{24}{5} \left(1 - \frac{M^2}{s} \right) \frac{M^2}{s} \frac{M^2}{s} \frac{1}{s} \log \frac{1 + \sqrt{1 - \frac{M^2}{s}}}{1 - \sqrt{1 - \frac{M^2}{s}}} \right]; \quad (3.8)$$

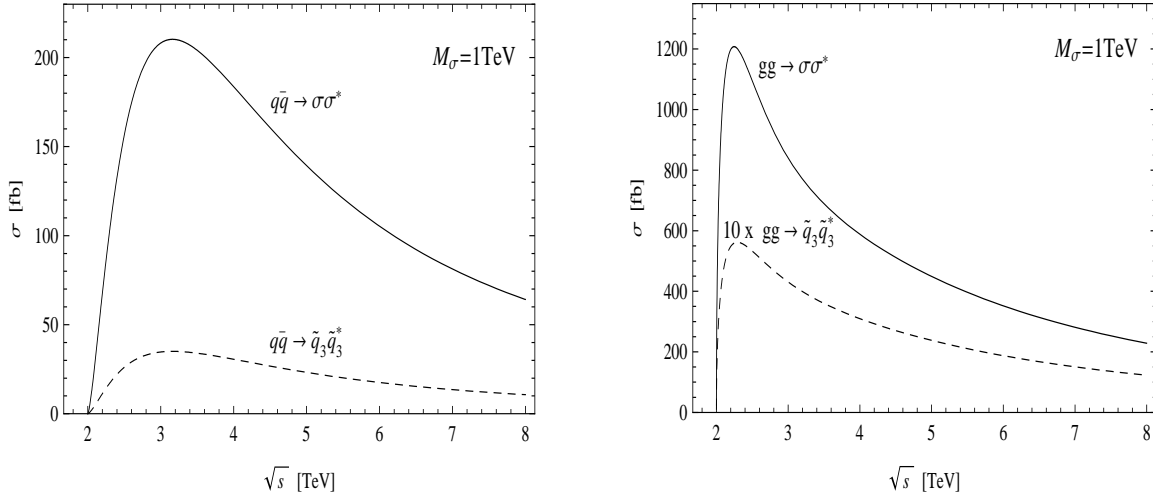


Figure 4: Parton cross sections for σ production in the qq (Left) and gg (Right) channel. For comparison, the production of 3rd generation squark pairs is shown by the dashed lines for the same masses.

The standard notation has been adopted for the parameters: \sqrt{s} is the invariant parton-parton energy, and M and $\beta = (1 - 4M^2/s)^{1/2}$ the mass and center-of-mass velocity of the particle. The QCD coupling is inserted to leading order, $\alpha_s(Q^2) = \alpha_s^{(5)}(Q^2) [1 + \beta_1^{(5)}(Q^2) + \beta_2^{(5)}(Q^2) \log^2(Q^2)]^{-1}$, where $\alpha_s^{(5)}(Q^2)$ evolves from $\alpha_s^{(5)}(M_Z^2) \approx 0.120$ with $N_F = 5$ flavors by definition, while the top-quark threshold is accounted for explicitly and supersymmetric particles do not affect the running in practice; the renormalization scale for the parton subprocesses is set to $Q = M$.

While the quark-annihilation cross section increases near threshold with the third power β^3 of the sgluon velocity, as characteristic for P-wave production, the cross section for equal-helicity gluon-fusion increases steeply with the velocity, as predicted for S-waves by the available phase space. Asymptotically the two parton cross sections scale $\propto s^{-1}$.

The cross sections are compared in Fig. 4 with the production of squark pairs [of the 3rd generation to match the dynamical production mechanisms]: $gg; qq \rightarrow \tilde{q}_3 \tilde{q}_3^*$. As expected, the cross sections exceed the $\tilde{q}_3 \tilde{q}_3^*$ cross sections by a large factor, i.e. ~ 20 for gg collisions and 6 for qq collisions. This can be exemplified by considering the evolution of ratios for the cross sections from small to maximum velocity, being again the center-of-mass velocity of the sgluon or squark in the final state:

$$\frac{[gg]}{[gg]_{\tilde{q}_3 \tilde{q}_3^*}} = \frac{\text{tr} [F^a F^a; F^b g F^a; F^b g]}{\text{tr} [\frac{a}{2}; \frac{b}{2}; \frac{a}{2}; \frac{b}{2}]} = \frac{216}{28=3} \approx 23 \quad \text{for } \beta \rightarrow 0; \tag{3.9}$$

$$\frac{[gg]}{[gg]_{\tilde{q}_3 \tilde{q}_3^*}} = \frac{\text{tr} (2F^a F^b F^b F^a + F^a F^b F^a F^b)}{\text{tr} [2\frac{a}{2} \frac{b}{2} \frac{b}{2} \frac{a}{2} + \frac{a}{2} \frac{b}{2} \frac{a}{2} \frac{b}{2}]} = \frac{180}{10} = 18 \quad \text{for } \beta \rightarrow 1;$$

$$\frac{[qq]}{[qq]_{\tilde{q}_3 \tilde{q}_3^*}} = \frac{\text{tr} [\frac{a}{2} \frac{b}{2}] \text{tr} [F^a F^b]}{\text{tr} [\frac{a}{2} \frac{b}{2}] \text{tr} [\frac{a}{2} \frac{b}{2}]} = \frac{12}{2} = 6 \quad \text{for any } \beta; \tag{3.10}$$

The ratio (3.9) decreases monotonically as β increases but by no more than 20%. Most important is the ratio at the maximum of the gg cross sections where it is still close to the initial maximal value; this can easily be explained by observing that, in Feynman gauge, the leading contribution is generated by the quartic coupling. The differences in the color factors reflect the different strengths of the couplings in the fractional triplet $\mathbf{3} = 2$ and the integer octet $\mathbf{8}$ couplings of $SU(3)_C$ with $(F^a)_{bc} = if^{abc}$. The cross sections are shown in Fig. 4 for $M = 1$ TeV across the invariant energy range relevant for the LHC. The values of the maxima in the gg and qq channels are about 1 pb and 0.2 pb,

respectively, a typical size for such processes.

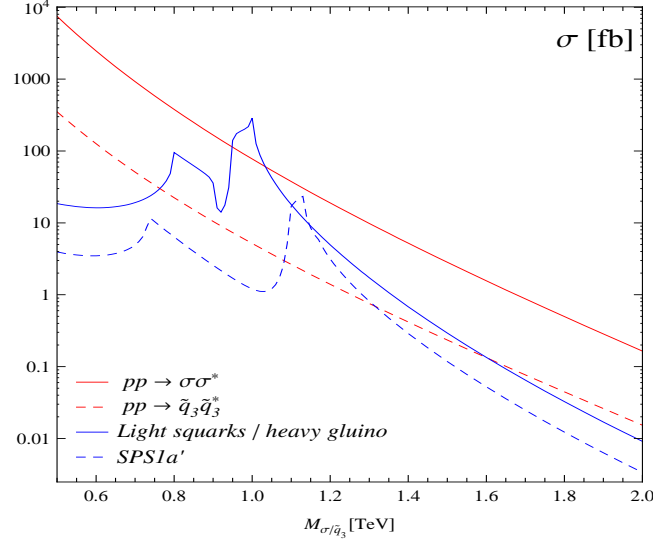


Figure 5: Cross sections for $\tilde{\chi}_1^0$ -pair [and \tilde{e}_β -pair] production (red lines), as well as for single $\tilde{\chi}_1^0$ production (blue lines), at the LHC. In the latter case the solid blue curve has been obtained using the same mass parameters as in Fig.2 (Right), while the dashed blue curve adopts the mSUGRA benchmark point SPS1a⁰.

The cross section for $\tilde{\chi}_1^0$ -pair production at LHC, $pp \rightarrow \tilde{\chi}_1^0 \tilde{\chi}_1^0$, is shown by the solid red curve in Fig.5 for the $m_{\tilde{\chi}_1^0}$ mass range between 500 GeV and 2 TeV [adopting the LO CTEQ6L parton densities [17]]. The cross section exceeds stop or sbottom $\tilde{\chi}_1^0$ -pair production (red dashed line), mediated by a set of topologically equivalent Feynman diagrams, by more than an order of magnitude, as anticipated at the parton level. With values from several picobarn downwards, a sizable event rate can be generated.

With the exception of $\tilde{\chi}_1^0 \rightarrow gg$ decays, all the modes shown in Fig.2 give rise to signatures that should be easily detectable if $m_{\tilde{\chi}_1^0}$ is not too heavy. The most spectacular signature results from $\tilde{\chi}_1^0 \rightarrow \tilde{g}\tilde{g}$ decay, each \tilde{g} decaying into at least four hard jets and two invisible neutralinos as LSP's. $\tilde{\chi}_1^0$ -pair production then generates final states with a minimum of eight jets and four LSP's, as noted in the Introduction.

The transverse momenta of the hard jets produced in the simplest case $\tilde{\chi}_1^0 \rightarrow \tilde{g}\tilde{g}$ can easily be estimated by analyzing production and decays near the mass thresholds, i.e. $M_{\tilde{\chi}_1^0} \approx 2m_{\tilde{g}} \approx 2m_{\tilde{q}} \approx m_{\tilde{\chi}_1^0}$. In this kinematic configuration the total jet transverse energy and the average jet transverse energy amount to

$$\langle E_{\tilde{\chi}_1^0}^{\text{tot}} \rangle \approx 2m_{\tilde{q}} \quad \text{and} \quad \langle E_{\tilde{\chi}_1^0} \rangle \approx m_{\tilde{q}} \quad (3.11)$$

The total transverse energy E_T carried by the LSPs and the vector sum of the momenta of the four $\tilde{\chi}_1^0$ in the final state, which determines the measured missing transverse momentum p_T , are predicted to be

$$\langle E_{\tilde{\chi}_1^0}^{\text{tot}} \rangle \approx 2m_{\tilde{q}} \quad \text{and} \quad \langle p_T \rangle \approx m_{\tilde{q}} \quad (3.12)$$

in the random-walk approximation for the $\tilde{\chi}_1^0$ momenta in the transverse plane. This is to be contrasted to gluino-pair production near threshold, where the corresponding observables are for the same mass configuration:

$$\tilde{g}\tilde{g} : \langle E_{\tilde{\chi}_1^0}^{\text{tot}} \rangle \approx m_{\tilde{q}} \quad \text{and} \quad \langle E_{\tilde{\chi}_1^0} \rangle \approx m_{\tilde{q}} \quad (3.13)$$

$$\langle E_{\tilde{\chi}_1^0}^{\text{tot}} \rangle \approx m_{\tilde{q}} \quad \text{and} \quad \langle p_T \rangle \approx \frac{p_{\tilde{q}}}{2} \quad (3.14)$$

Thus, the total jet transverse energies and the missing transverse momenta are markedly different in the N=1 and N=2 theories for the same mass configurations.

These simple estimates are backed up by a Monte-Carlo simulation of \tilde{g} -pair production at the LHC, followed by the decay into four on-shell gluinos. The total transverse jet energy and the vector sum of the LSP transverse momenta are summarized in Tab.I for a spectrum of $m_{\tilde{g}}$ masses, and fixed ratios of gluino, squark and LSP neutralino masses. The squark and gluino masses are again chosen at about half a TeV. The values of the transverse momenta match the earlier estimates quite well. It should be noted however that the jet transverse momenta fall into two groups. The transverse momenta of jets in gluino to squark decays are generally small while the transverse momenta of the jets generated in squark decays are large. Both groups are populated equally so that the average transverse momenta of the jets are reduced by an approximate factor two compared with the MSSM gluino pair production [setting $m_{\tilde{g}} = M_{\tilde{g}}^{\text{hybrid model}}$ for the proper comparison].

Table I: Transverse jet energies and vector sum of the LSP transverse momenta for final states in $2\tilde{g}$ and $2\tilde{g}$ production, with primary $m_{\tilde{g}}$ masses of 1.5 and 0.75 TeV; the mass hierarchy in the cascade decays is noted in the bottom line. Below the transverse energy per jet of the total jet ensemble [tot], the transverse energies in the high and the low jet-energy groups [high/low] are displayed. All quantities in TeV.

$M_{\tilde{g}}$	$2\tilde{g}$		$2\tilde{g}$		$2\tilde{g}$	
	$E_{\tilde{g}}^{\text{tot}}$	$E_{\tilde{g}}$	$E_{\tilde{g}}^{\text{tot}}$	$E_{\tilde{g}}$	$E_{\tilde{g}}$	$E_{\tilde{g}}$
1.50 TeV [tot]	1.67	0.21	1.67	0.42	0.45	0.65
[high]		0.27		0.53		
[low]		0.15		0.31		
0.75 TeV [tot]	0.91	0.11	0.93	0.23	0.22	0.31
[high]		0.14		0.29		
[low]		0.08		0.17		
$M_{\tilde{g}} = 2M_{\tilde{g}} = 8=3M_{\tilde{g}} = 15M_{\tilde{g}}$						

Other interesting final states resulting from \tilde{g} -pair production are four-stop states $\tilde{t}_1\tilde{t}_1\tilde{t}_1\tilde{t}_1$, which can be the dominant mode if $m_{\tilde{g}} > m_{\tilde{g}}$ and L-R mixing is significant in the stop sector, and $\tilde{q}\tilde{q}\tilde{g}\tilde{g}$, which can be a prominent mode if $M_{\tilde{g}} > 2m_{\tilde{g}} + 2m_{\tilde{q}}$. These channels also lead to four LSPs in the final state, plus a large number of hard jets. On the other hand, the $\tilde{t}\tilde{t}\tilde{t}\tilde{t}$ final state, which can be the dominant mode if the two-body decays into squarks and gluinos are kinematically excluded, might allow the direct kinematic reconstruction of $M_{\tilde{g}}$.

3.3. Single Channel

As noted earlier, gluons can be generated singly in gluon-gluon collisions via squark loops. The partonic cross section, with the Breit-Wigner function factorized out, is given by

$$\hat{\sigma}[\tilde{g} \rightarrow \tilde{g}] = \frac{2}{M_{\tilde{g}}^3} (\Gamma_{\tilde{g}} \rightarrow \tilde{g}\tilde{g}); \quad (3.15)$$

where the partial width for $\tilde{g} \rightarrow \tilde{g}\tilde{g}$ decays has been given in Eq. (3.2).

The resulting cross section for single \tilde{g} production at the LHC is shown by the blue curves in Fig.5 [based on the LO CTEQ6L parton densities [17]]. The solid curve has been calculated for the parameter set of the right frame of Fig.2, while the dashed curve has been determined by taking the soft breaking parameters in the gluino and squark sector from the widely used benchmark point SP S1a⁰ [18]. In the former case the single \tilde{g} cross section can exceed the \tilde{g} -pair production cross section for $M_{\tilde{g}} > 1$ TeV. Since SP S1a⁰ has a somewhat smaller gluino mass [which we again interpret as a Dirac mass here] it generally leads to smaller cross sections for single \tilde{g} production. Taking $m_{\tilde{g}} = 2M_{\tilde{g}}^{\text{D}}$ as in the left frame of Fig.2, would lead to a very small single \tilde{g} production cross section. Recall that

$m_{\tilde{q}} > M_{\tilde{D}}^{\tilde{D} \rightarrow j}$ is required if $\tilde{t} \rightarrow t\tilde{t}$ decays are to dominate. We thus conclude that one cannot simultaneously have a large $\sigma(pp \rightarrow \tilde{t})$ and a large $\text{Br}(\tilde{t} \rightarrow t\tilde{t})$.

The signatures for single \tilde{t} production, which is an $\mathcal{O}(\alpha_s^3)$ process, are potentially exciting as well. However, since all final states resulting from \tilde{t} decay can also be produced directly in tree-level $\mathcal{O}(\alpha_s^2)$ processes at the LHC, it is a problem to be solved by experimental simulations whether single \tilde{t} production is detectable as a resonance above the SM plus MSSM backgrounds, given that in most cases, with the exception of the 2-gluon channel, the direct kinematic reconstruction of $M_{\tilde{t}}$ is not possible.

4. SUMMARY

The color-octet scalar sector in the $N=1/N=2$ hybrid model we have analyzed in this letter, leads to spectacular signatures of supersymmetry which are distinctly different from the usual MSSM topologies. Depending on the masses of the particles involved, either multi-jet final states with high sphericity and large missing transverse momentum are predicted, or four top quarks should be observed in $2\tilde{t}$ production. If the mass splitting between L and R squarks is not too small, loop-induced single \tilde{t} production may also have a sizable cross section; however, this channel suffers from much larger backgrounds, though identifying the \tilde{t} particle as a resonance in 2-gluon final states would truly be an exciting experimental observation.

In this letter we assumed that gluinos are pure Dirac states, and that the two components of the complex scalar field, $\tilde{g} = (S + iP)\sqrt{2}$, are degenerate. Relaxing these assumptions would introduce more parameters into the scheme, yet the central characteristics of the experimental event topologies of the final states at LHC would not change significantly. For example, for fixed mass, the S or P pair production cross section is simply half the $\tilde{g}\tilde{g}$ pair production cross section.

Acknowledgments

The work by SYC was supported by the Korea Research Foundation Grant funded by the Korean Government (MOERHRD, Basic Research Promotion Fund) (KRF-2008-521-C00069). The work of MD was partially supported by Bundesministerium für Bildung und Forschung under contract no. 05HT6PDA, and partially by the Marie Curie Training Research Networks "UniverseNet" under contract no. MRTN-CT-2006-035863, "ForcesUniverse" under contract no. MRTN-CT-2004-005104, as well as "The Quest for Unification" under contract no. MRTN-CT-2004-503369. JK was supported by the Polish Ministry of Science and Higher Education Grant no 1P03B 108 30 and the EC Programme "Particle Physics and Cosmology: the Interface" under contract no. MTKD-CT-2005-029466. PMZ is grateful for the warm hospitality extended to him at the Inst. Theor. Phys. E of RWTH Aachen, and at LPT/Orsay of Paris-Sud. We are particularly thankful to T. Plehn and T. Tait for their cooperation in clarifying the origin of discrepancies between their first version Ref. [8] with our results.

-
- [1] Yu. A. Golfand and E. P. Likhtman, JETP Lett. 13 (1971) 3214; J. Wess and B. Zumino, Nucl. Phys. B 70 (1974) 39.
 [2] H. P. Nilles, Phys. Rept. 110 (1984) 1; H. E. Haber and G. L. Kane, Phys. Rept. 117 (1985) 75.
 [3] M. Drees, R. Godbole and P. Roy, "Theory and phenomenology of sparticles: An account of four-dimensional $N=1$ supersymmetry in high energy physics," Hackensack, USA: World Scientific (2004) 555 p; P. Binetruy, "Supersymmetry:

- Theory, experiment and cosmology," Oxford, UK : Oxford Univ. Pr. (2006) 520 p; J. Wess and J. Bagger, Princeton, USA : Univ. Pr. (1992) 259 p.
- [4] P. Fayet, Nucl. Phys. B 113 (1976) 135; L. Alvarez-Gaume and S.F. Hassan, Fortsch. Phys. 45 (1997) 159 [arXiv:hep-th/9701069].
- [5] S.Y. Choi, M. Drees, A. Freitas and P.M. Zerwas, Phys. Rev. D 78 (2008) 095007 [arXiv:0808.2410 [hep-ph]].
- [6] K. Benakli and C. Moura, in M. M. Nojiri et al., arXiv:0802.3672 [hep-ph].
- [7] M. M. Nojiri and M. Takeuchi, Phys. Rev. D 76 (2007) 015009 [arXiv:hep-ph/0701190].
- [8] T. Plehn and T.M.P. Tait, arXiv:0810.3919 [hep-ph] and corrected version [in preparation].
- [9] Z. Chacko, P.J. Fox and H.M. Urayama, Nucl. Phys. B 706 (2005) 53 [arXiv:hep-ph/0406142]; A.V.M. Anohar and M.B. Wise, Phys. Rev. D 74 (2006) 035009 [arXiv:hep-ph/0606172]; I. Antoniadis, K. Benakli, A. Delgado and M. Quiros, Adv. Stud. Theor. Phys. 2 (2008) 645 [arXiv:hep-ph/0610265]; M.I. Gresham and M.B. Wise, Phys. Rev. D 76 (2007) 075003, arXiv:0706.0909 [hep-ph]; M. Gorbush, T.J. Khoo, D.J. Phalen, A. Pierce and D. Tucker-Smith, Phys. Rev. D 77, 095003 (2008), arXiv:0710.3133 [hep-ph]; G.L. Kane, A.A. Petrov, J. Shao and L.T. Wang, arXiv:0805.1397 [hep-ph]; M.V. Martsynov and A.D. Smimov, Mod. Phys. Lett. A 23, 2907 (2008), arXiv:0807.4486 [hep-ph]; B.K. Zur, L. Mazucato and Y. Oz, JHEP 0810 (2008) 099, arXiv:0807.4543 [hep-ph]; P. Fileviez Perez, R. Gavin, T. McElmurry and F. Petriello, arXiv:0809.2106 [hep-ph]; C. Kilic, S. Schumann and M. Son, arXiv:0810.5542v1 [hep-ph]; C. Kim and T. Mehen, arXiv:0812.0307 [hep-ph].
- [10] P.J. Fox, A.E. Nelson and N. Weiner, JHEP 0208 (2002) 035 [arXiv:hep-ph/0206096].
- [11] A.E. Nelson, N. Rius, V. Sanz and M. Utsal, JHEP 0208 (2002) 039 [arXiv:hep-ph/0206102].
- [12] I. Antoniadis, J.R. Ellis and G.K. Leontaris, Phys. Lett. B 399 (1997) 92 [arXiv:hep-ph/9701292]; G.D. Kribs, E. Poppitz and N. Weiner, arXiv:0712.2039 [hep-ph].
- [13] J.F. Gunion and H.E. Haber, Nucl. Phys. B 278 (1986) 449.
- [14] G. Passarino and M. Veltman, Nucl. Phys. B 160 (1979) 151.
- [15] W. Beenakker, R. Hopker, M. Spira and P.M. Zerwas, Nucl. Phys. B 492 (1997) 51 [arXiv:hep-ph/9610490].
- [16] S. Dawson, E. Eichten and C. Quigg, Phys. Rev. D 31 (1985) 1581.
- [17] J. Pumplin, D.R. Stump, J. Huston, H.L. Lai, P.M. Nadolsky and W.K. Tung, JHEP 0207 (2002) 012 [arXiv:hep-ph/0201195].
- [18] J.A. Aguilar-Saavedra et al., Eur. Phys. J. C 46 (2006) 43 [arXiv:hep-ph/0511344].